https://doi.org/10.5194/essd-2026-202
Preprint. Discussion started: 15 April 2026

Open Access Earth System Science Data Discussions

Ground-Motion Dataset for Shallow Earthquakes in Colombia

Daniel Martinez-Jaramillo[1,2], Sreeram-Reddy Kotha[3], F. Ramón Zúñiga[4], Pierre Lacan[4].

[1]Posgrado en Ciencias de la Tierra, Instituto de Geociencias, Universidad Nacional Autónoma de México. Querétaro, 76230, México.

[2]Now at Servicio Geológico Colombiano. Observatorio Vulcanológico y Sismológico de Pasto, 520002, Nariño, Colombia.

[3]Institut des Sciences de la Terre, Université Grenoble Alpes, Grenoble, 38400, France.

[4]Instituto de Geociencias, Universidad Nacional Autónoma de México. Juriquilla, 76230, Querétaro, México.

Correspondence to: Daniel Martinez-Jaramillo (dmartinezj@sgc.gov.co)

Abstract. The tectonics of Colombia is characterised by the interaction of multiple oceanic plates subducting beneath the continent, generating active transpressional deformation and a wide range of subduction-related and crustal earthquakes. We present a flatfile containing ground-motion intensity measurements from 694 shallow earthquakes. The dataset includes 8,086 three-component acceleration records that were uniformly processed. The computed IMs include peak ground velocity, peak ground acceleration, and 5%-damped spectral accelerations for 31 periods ranging from 0.01 to 8 s. Furthermore, the Fourier Amplitude Spectra for each component is provided in the frequency range from 0.04 to 30 Hz. Epicentral and hypocentral distances are reported for all events, while finite-fault distance metrics are estimated for earthquakes with M > 5.5. Site conditions are characterised using V_{S30} and the horizontal-to-vertical spectral ratio (H/V). Hypocentre locations are constrained using the ISC-EHB catalogue and the Integrated Seismological Catalogue of the Colombian Geological Survey. For validation and consistency checks, the dataset was compared to a global and region-adapted Ground Motion Prediction Model. This flatfile constitutes a valuable resource for seismic hazard analysis, ground-motion modelling, risk assessment, earthquake engineering applications, seismic-site response and source physics characterization in Colombia, surrounding regions, and other comparable tectonic environments.

1 Introduction

The subduction of the Nazca and Caribbean plates, together with the indention (or possible additional subduction) of the Panamá-Chocó block against the northwestern South American plate, generates moderate to large earthquakes in the region. As a result, Colombia experiences a complex mixture of interface, intraslab, shallow continental, lithospheric continental, and volcanic-related earthquakes. Several significant earthquakes have strongly affected Colombia, for example:

- 18 May 1875, ***M*** 6.8, in Cúcuta, Norte de Santander, occurred near the Colombia–Venezuela border, causing approximately 1,000 fatalities. The likely source is the Aguas Calientes Fault System, part of the Boconó Fault System in the Mérida Andes (Rodríguez et al., 2018).

https://doi.org/10.5194/essd-2026-202
Preprint. Discussion started: 15 April 2026

- 31 January 1906, ***M*** 8.8 in the Colombia–Ecuador border, a megathrust event along the Nazca subduction zone that generated a devastating tsunami and caused around 600 fatalities - one of the largest earthquakes recorded globally.
- 12 December 1979, ***M*** 8.2 (Tumaco, Nariño): Another major subduction earthquake that caused a tsunami and a death toll of more than 450.
- 31 March 1983, ***M*** 5.5 (Popayán, Cauca): Caused approximately 300 fatalities; the source is attributed to one of the structures belonging to the Romeral Fault System (RFS) (Marín-Árias et al., 2006).
- 18 October 1992, ***M*** 7.2, Murindó, Antioquia, caused more than 10 fatalities and widespread environmental effects, including soil liquefaction. This earthquake is associated with the Murindó Fault (Paris et al., 2000; Marín et al., 2009; Mosquera-Machado et al., 2009).
- 25 January 1999, ***M*** 6.1 (Eje Cafetero): Produced more than 2,000 deaths and has been linked to the Córdoba Fault of the RFS (Paris et al., 2000; Vargas-Jiménez & Monsalve-Jaramillo, 2009).

This brief set of examples highlights the importance of characterizing and quantifying the intensity caused by shallow crustal earthquakes in Colombia. Globally, several major initiatives have undertaken the compilation and processing of seismograms to make ground-motion IMs widely available. These include the Next Generation Attenuation (NGA) projects for Western (NGA-West2) and Eastern U.S. (Ancheta et al., 2012; Goulet et al., 2021), the Near-Source Ground-motion Flatfile (Pacor et al., 2018; Sgobba et al., 2021), and regional efforts covering Europe (Akkar et al., 2014; Lanzano, 2020), Italy (Oliveti et al., 2021), France (Buscetti et al. 2025), Belgium (Vanneste et al. 2026), India (Sharma et al., 2025), Japan (Dawood et al., 2016), and Chile (Bastías & Montalva, 2016) among others.

For Northern South America, Arteta et al. (2021) developed a GMPM for subduction earthquakes, Arteta et al. (2023) developed a GMPM for shallow crustal earthquakes with 709 records of 56 earthquakes, also Pájaro et al. (2024) developed a GMPM for the Bucaramanga Nest.

The accessibility of IMs for a wide [***M, R***] ranges is essential for the development of GMPMs, probabilistic seismic hazard assessment (PSHA), engineering seismology, and earthquake engineering. The development of GMPMs, particularly the partially non-ergodic kind, relies heavily on the quantity and quality of ground-motion IMs, and associated event, path, and site metadata. Such datasets are often referred to as *flatfiles*. Here, we present a flatfile generated from consistently processed ground-motion recordings from the shallow earthquakes across Colombia and tested with a global and a region-adapted GMPM for consistency check purposes.

2 Compilation of the Data

The flatfile is arranged as a table that contains verified and reliable metadata and IMs of processed waveforms recorded by the SGC. SGC provided, upon request, more than 10,000 quality-checked acceleration time series. Earthquake criteria selection to the flatfile from SGC database was:

- Events in the latitude range 0º to 14ºN;
- Events in the longitude range 69ºW, 82ºW;
- Events with depth estimation < 50 km;
- ***M*** > 4;
- Records with R_{epi} < 400 km.

https://doi.org/10.5194/essd-2026-202
Preprint. Discussion started: 15 April 2026

Open Access Earth System Science Data Discussions

SGC is a national network consisting of 506 seismological and accelerometric stations operating since 1993 installed around Colombia; some of them were removed or operated in temporary networks. The FDSN code for this network is CM. In addition, there are local networks within the country to specifically monitor volcanoes, mining districts, and oil and gas fields; some of these stations were shared with SGC and contributed to this flatfile. The sampling frequency of accelerometric stations is predominantly 200 Hz, with a few stations (3) at 100 Hz.

2.1 Flatfile structure

The fields of flatfile are grouped as: (1) Event metadata; (2) Site metadata; (3) Metrics of event-to-site distances; (4) Intensity measures.

The 694 events are defined by their location (Latitude, Longitude, depth), origin time (date), and magnitude. Magnitudes were taken from the Integrated Seismic Catalog for Colombia (Montejo et al., 2023). This catalog was reviewed for locations and homogenized in magnitude. For the events not included in the dataset of Montejo et al. (2023), we followed the same criteria, prioritizing locations made by ISC-EHB (Weston et al., 2016) and SGC. Moment-magnitudes were compiled from the Global CMT catalog (Ekström et al., 2012), USGS-NEIC, ISC mb, and SGC M_L. Focal mechanisms were taken from GCMT and SGC. Geometry of the rupture plane is a simple description from the nodal plane preferred for the focal mechanism selected by the authors of this dataset from the geological context, with strike, dip, and rake for slip kinematics.

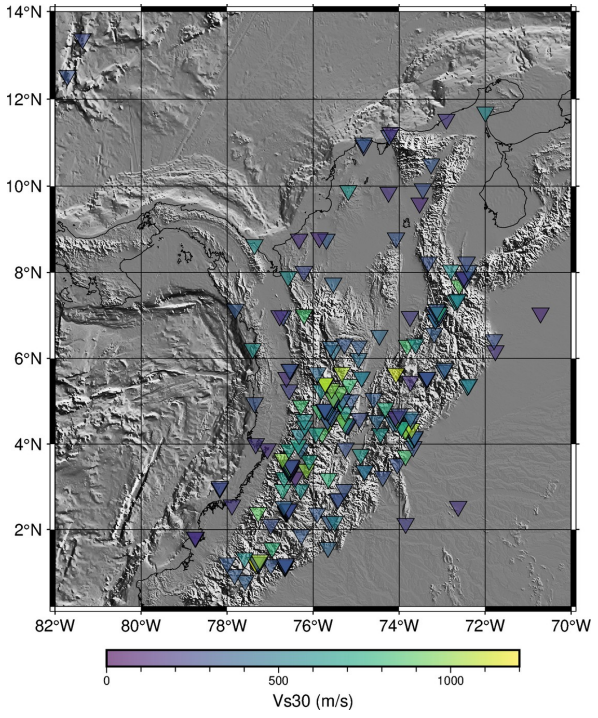

Figure 1. Sites used in this work and V_{S30}.

Moment-magnitude (***M***) is the preferred magnitude in GMPMs and PSHA. Magnitude range is 3.5 to 7.2. When ***M*** was not available, m_b or M_L values were taken depending on availability. To homogenize these magnitudes into

https://doi.org/10.5194/essd-2026-202
Preprint. Discussion started: 15 April 2026

Open Access Earth System Science Data Discussions

M, we applied the conversion relationships calibrated specifically for the Colombian territory by SGC & GEM (2018):

Relationship	σ
$M = 0.954\, m_b + 0.42 \; for \; 3.6 < m_b < 5.7$	0.28
$M = 1.433\, m_b - 2.35 \; for \; 5.7 < m_b < 7.7$	0.36
$M = 0.958\, M_L + 0.1 \; for \; 2.9 < M_L < 6.1$	0.50

Table 1. Equations used to homogenize moment magnitude (***M***) from SGC & GEM (2018).

The 227 sites featured in this dataset have been installed, maintained, and administered by SGC (Figure 1). The site parameters used in this dataset is the *inferred* time-averaged shear-wave velocity in the upper 30 m of soil (V_{S30}), taken from the map of V_{S30} for Colombia (Eraso and Montejo, 2019), which were derived from topographic slope. Measures of the H/V in the Fourier domain (HVFSR) and pseudo-spectral acceleration (HVRSR) were published by Mercado et al. (2024) for sites in north-western South America. 154 of the 227 sites in the flatfile are present in the Mercado et al. (2024) dataset. In-situ measurements of Mercado et al. (2024) coincide with 28 sites of this dataset for which microtremor-based shear velocity profiles, H/V from FAS of microtremor analysis (mHVFSR), and *measured* V_{S30} are available. The predominant period of the site (T_0) is also taken from Mercado et al. (2024).

Epicentral (R_{epi}) and hypocentral (R_{hyp}) distances and Azimuth are reported for the entire dataset, whereas extended rupture-based distances (R_{rup}, R_{JB}, R_x, R_{y0}) were computed only for earthquakes with ***M*** > 5.5. These distances were computed from the geometry of the rupture plane derived from the preferred nodal plane. Rupture dimensions were computed following Strasser et al. (2010) for subduction interphase-related earthquakes and following Wells and Coppersmith (1994) for continental events. The hypocenter was placed at the midpoint of the fault plane, but for earthquakes with hypocentral depths shallower than 10 km, the midpoint of the rupture plane was placed at 12.5 km depth as the average thickness of the seismogenic depth. Joyner-Boore distance (R_{JB}) was computed as the closest horizontal distance from the site to the surface projection of the rupture plane. R_x represents the horizontal distance from the top edge of the rupture measured perpendicular to the fault strike, with positive and negative values indicating sites on the hanging-wall ($R_x > 0$) and footwall ($R_x < 0$) sides, respectively. R_{y0} is the horizontal distance measured parallel to the strike from the fault midpoint.

For the **waveform** processing, we followed the steps presented by Paolucci et al. (2010) and Lanzano et al. (2019):

1. Baseline correction;
2. Cosine taper;
3. Application of a second order acausal bandpass Butterworth filter to the acceleration time-series;
4. Double integration to obtain displacement time series;
5. Linear detrending of the displacement;
6. Double differentiation to get the corrected acceleration.

https://doi.org/10.5194/essd-2026-202
Preprint. Discussion started: 15 April 2026

For the bandpass filter limits, we used median values from Lanzano et al. (2019). As they pointed out, the low-pass filter frequency (f_{lp}) is magnitude independent, we took the mean value of 32.26 Hz, while for the high pass (f_{hp}) filter we used a magnitude-dependent function as:

$$f_{hp} = 0.15\ Hz\ for\ M < 4$$
$$f_{hp} = -0.05(M) + 0.35\ Hz\ 6 \geq M \geq 4 \quad (1)$$
$$f_{hp} = 0.05\ Hz\ for\ M > 6.$$

We test the sensitivity of the parameter RotD50 PGA with the fixed f_{lp} of the bandpass filter at 32.26 Hz, taking the records and changing f_{lp} in a range of 27 to 37 Hz. The sensitivity analysis shows that most records are weakly affected by the choice of f_{lp}, as the average variation is 2.31% and the 90th quantile is 7.0%. However, 6.4% of the recordings exhibit variation larger than 10% in RotD50 PGA. These records are concentrated around ***M*** 4.5 and R_{epi} > 250 km (Figure A1). These differences are likely related to high-frequency signal content or noise close to the selected filter corner frequency, which could affect the peak acceleration amplitude.

FAS from the acceleration records in the three components are computed in the frequency range 0.04 to 30 Hz, applying Konno and Ohmachi (1998) function with smoothing (Lanzano et al. 2019). An example of FAS computed for an ***M*** 6.1 earthquake recorded at 13 km is shown in Figure 2.

Usable frequencies are limited to those between the high-pass and low-pass by a safety factor of 1.25 to ensure that the filters do not have a significant effect on the response spectral values (Abrahamson and Silva, 1997). Hence, the usable bandwidth decreases at low frequencies for small magnitudes, and the upper limit for our dataset is 25.808 Hz. Lowest usable frequencies (LUF) are:

$$LUF = 0.1875\ Hz\ for\ M < 4,$$
$$LUF = -0.0625(M) + 0.4375\ Hz\ for\ 6 \geq M \geq 4, \quad (2)$$
$$LUF = 0.0625\ Hz\ for\ M > 6.$$

A compilation of Effective Amplitude Spectrum (EAS) (Kottke et al. 2018), defined in equation 3, binned by magnitude, is shown in Figure 3.

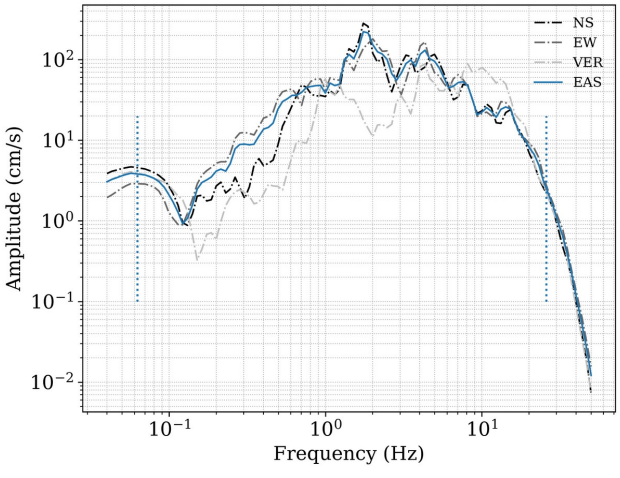

https://doi.org/10.5194/essd-2026-202
Preprint. Discussion started: 15 April 2026

Open Access Earth System Science Data Discussions

Figure 2. Fourier amplitude spectrum recorded by each component at ARMEC. Earthquake occurred on January 25, 1999 with ***M*** = 6.1. Dotted vertical blue lines represent bandwidth limits of the usable spectra for this earthquake.

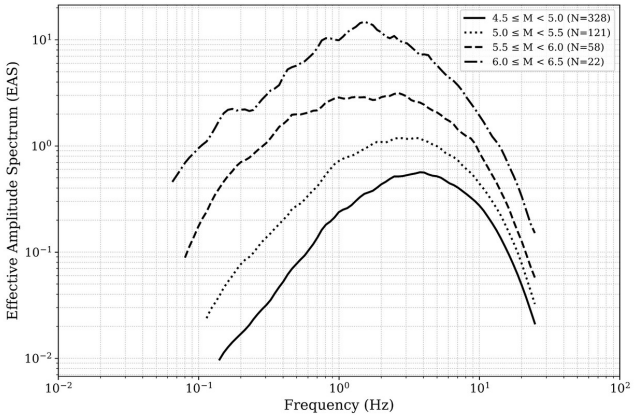

Figure 3. Fourier amplitude spectrum geometric mean of the horizontal components (EAS) is binned by magnitudes for records with R_{epi} < 100 km. The limits of usables frequencies in function of magnitude can be appreciated.

The dataset includes IMs that are independent of sensor orientation, calculated using the median and maximum spectral ordinates over all non-redundant horizontal orientations, RotD50 and RotD100 (Boore, 2010), respectively. All spectral values were computed from the corrected accelerograms using standard response-spectrum analysis. Furthermore, the EAS is computed from the two horizontal components of FAS. The following IMs are provided:

- RotD50 Peak Ground Acceleration (PGA) for the horizontal components.
- PGA, PGV, and 5%-damped spectral accelerations for each of the north–south, east–west, and vertical components.
- RotD50 spectral accelerations for 5% damping and oscillator periods ranging from 0.010 s to 8.0 s.
- Amplitudes of the Fourier Spectrum in the range 0.04 to 30 Hz for the three components.
- EAS defined as

$$EAS(f) = \sqrt{\frac{1}{2}\left[FAS_{H1}(f)^2 + FAS_{H2}(f)^2\right]} \quad (3)$$

where H_1 and H_2 are the given horizontal components at f.

3 Data Statistics

The [***M, R***$_{epi}$] distribution of 8,086 records from 694 earthquakes in the catalogue is shown in Figure 4. Epicenters of 509 earthquakes are located in the continental territory, whereas 185 are located offshore of the Colombian coastline. The classification between tectonic environments, such as subduction interface and intraslab among others is left for user determination depending on the slab models and classification methods used.

https://doi.org/10.5194/essd-2026-202
Preprint. Discussion started: 15 April 2026

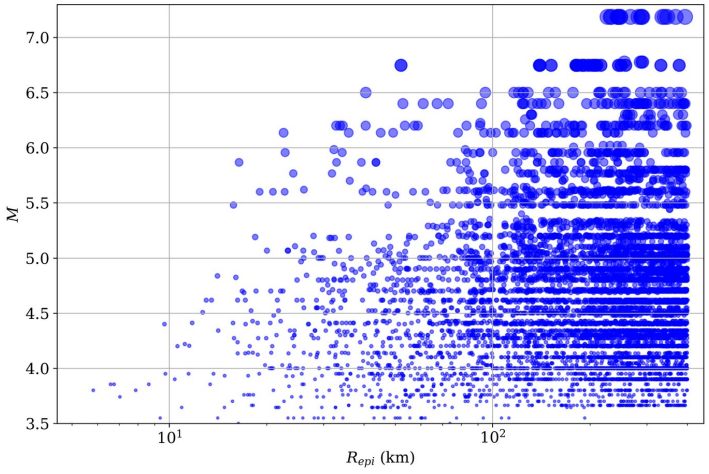

Figure 4. Distribution of ***M*** and distance of the 8,8086 records.

Data are sampled in the magnitude range 3.5 - 7.2 and for epicentral distances up to 400 km. There is also a significant number of records related to strong events with a magnitude greater than 5.5, corresponding to 8.9% of the records (716) from 42 earthquakes. In addition, there are 15 events with magnitudes larger than 6.0, such as the ***M*** 6.1 1999 Eje Cafetero earthquake, ***M*** 7.2 2004 Pizarro earthquake on the Pacific coast, and ***M*** 6.1 2023 San Juanito earthquake in eastern Colombia.

Figure 5 shows the number of records by R_{epi}, ***M***, depth, and V_{s30} in the dataset. Most of the data are relative to distances larger than 100 km (about 85%); 5.3% of the records correspond to distances shorter than 50 km. The distribution of recordings in terms of depth intervals shows that most of the data have focal depth lower than 20 km, corresponding to about 69% of the total records in the flatfile, thus indicating a predominance of shallow crustal events in the dataset. Indeed, about 2868 records (31%) correspond to 20 < depth (km) < 55.

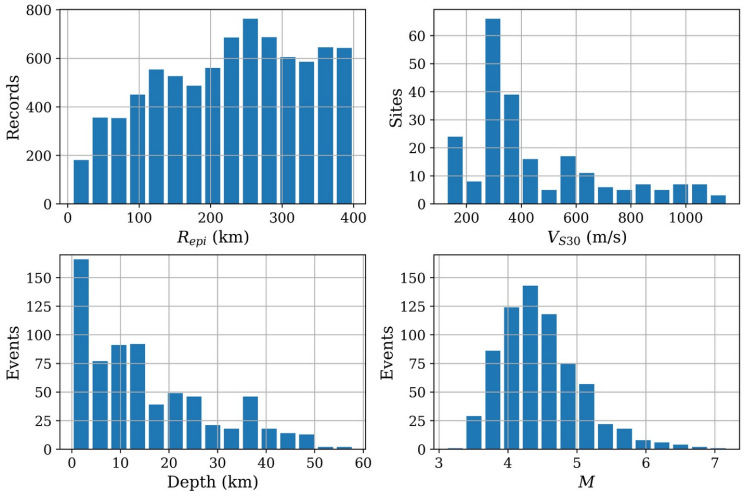

Figure 5. Histograms of the records used in the flatfile showing epicentral distance, V_{S30}, magnitude and focal depth of the earthquakes, records and sites used in the dataset.

https://doi.org/10.5194/essd-2026-202
Preprint. Discussion started: 15 April 2026

3.1 Consistency check: Residual analysis

For validation purposes (Bindi et al. 2019), we predicted PGA, SA (RotD50), and EAS IMs of the continental earthquakes in our dataset (509 events) – to compute residuals (equation 4) – using the input parameters in the GMPM.

The GMPM used here are the global development of Abrahamson et al. (2014) – made with the NGA-West 2 dataset – and the one of Areteta et al. (2023), which is a regional development for Northern South America of Abrahamson et al. (2014).

The comparison between observed and predicted IMs provides a consistency check for the data quality and processing methodology as shown in Figure 6, where the total residual (δ_{total}) is plotted against R_{epi} and ***M***, without significant biases.

The δ_{total} can be decomposed into between-event (δB_e), between-site ($\delta S2S_s$), and leftover residuals (ε) (Al Atik et al., 2010) as:

$$y_{es}(T) = u_{es}(M, R_{es}, V_{S30}, T) + \delta B_e + \delta S2S_s + \varepsilon \quad (4)$$

where y is the natural logarithm of the observed IMs from an individual earthquake, e, with magnitude ***M*** observed at site, s, with V_{S30} located at a distance R_{es}. u_{es} is the predicted median IMs from the GMPM.

The total standard deviation of the GMPM (σ) can be written as:

$$\sigma = \sqrt{\boldsymbol{\tau}^2 + \phi_{S2S}^2 + \phi_0^2} \quad (5)$$

where $\boldsymbol{\tau}$, ϕ_{S2S}, ϕ_0 are the standard deviation of δB_e, $\delta S2S_s$ and ε respectively.

Following residual decomposition of equation (4), we get δB_e and $\delta S2S_s$ to show their distribution, results are shown in Figures 7 and 8, respectively, and compiled in Table 2.

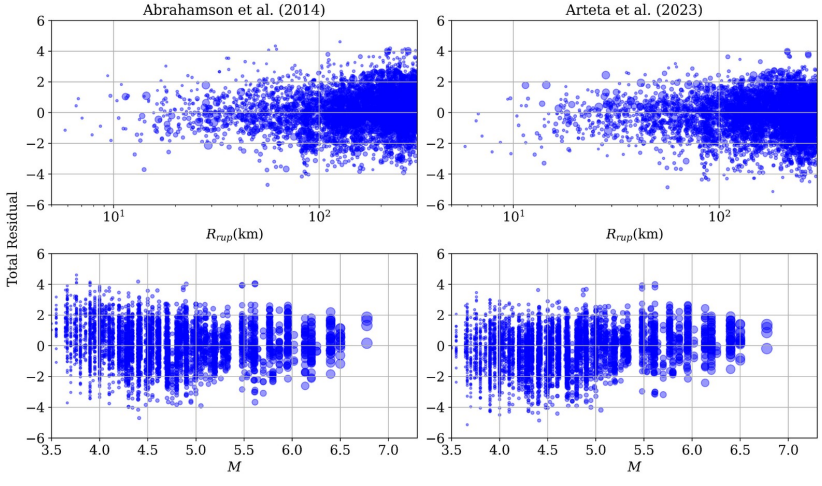

Figure 6. Scatterplots of the total residual of the RotD50 PGA of the continental earthquakes in the dataset vs. R_{rup} and ***M***. The left panel figures are computed from Abrahamson et al. (2014) and right panel figures are computed from Arteta et al. (2023).

GMPM	Abrahamson et al. (2014)	Arteta et al. (2023) (RotD50 PGA)	Bayless and Abrahamson (2018) (EAS 5 Hz)

https://doi.org/10.5194/essd-2026-202
Preprint. Discussion started: 15 April 2026

	(RotD50 PGA)		
Coverage	Global for SA	Regional for Northern South America for SA	Global for FAS
δ_{total} mean	0.162	-0.318	0.541
δ_{total} std	1.316	1.290	1.349
$\|\delta_{total}\| < 1$ * std	69.0 %	68.3 %	69.1%
$\|\delta_{total}\| < 2$ * std	95.6 %	95.3 %	95.6%
$\|\delta_{total}\| < 3$ * std	99.7 %	99.6%	99.7%
τ	0.95	0.88 (0.43)	0.92 (0.38)
ϕ_{S2S}	0.75	0.74	1.09 (0.40)
ϕ_0	0.68	0.67	0.56
σ	1.39	1.33	1.53

Table 2. Basic statistics and standard deviation of the residuals of the dataset from GMPM of Abrahamson et al. (2014), Arteta et al. (2023), and Bayless and Abrahamson (2018). In parentheses is shown the standard deviation from the publication in the original paper.

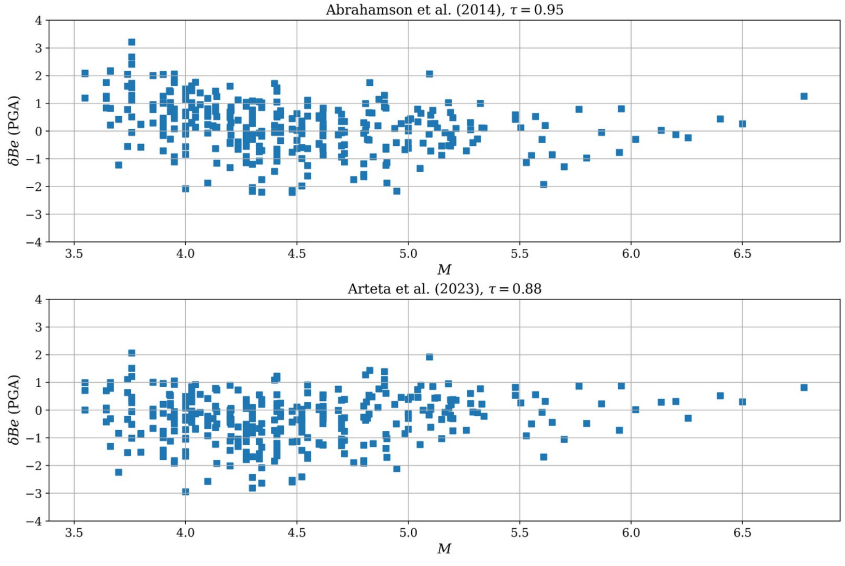

https://doi.org/10.5194/essd-2026-202
Preprint. Discussion started: 15 April 2026

Open Access Earth System Science Data Discussions

Figure 7. Between event variability (δBe) of the continental earthquakes in the dataset and its standar deviation (τ). δBe in the upper panel is computed with Abrahamson et al. (2014) while in the lower panel is computed with Arteta et al. (2023).

The trends of δBe showed a significant scatter for M < 4.5, which causes high τ; this could be related to the empirical relationships used in the conversion of Ml, Mb to M. One way to corroborate this could be the computation of M from the FAS values presented here, from the seismic moment taken from corner frequencies. Another approach could be to update the GMPM in a Bayesian framework with a larger range of small to medium-sized M.

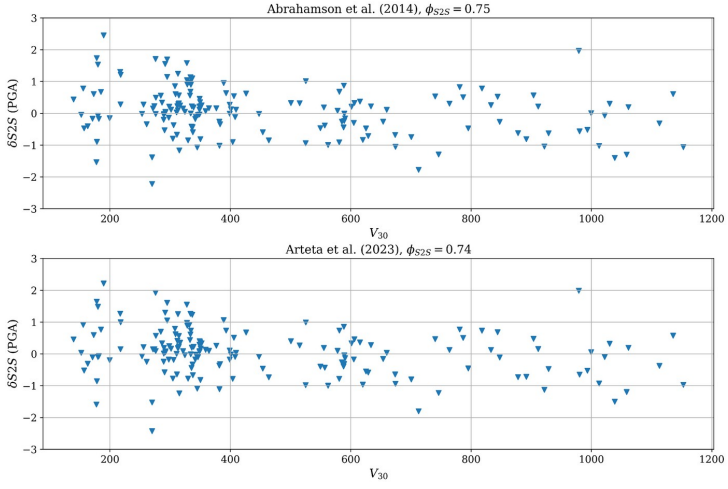

Figure 8. Site-to-site residuals ($\delta S2S_s$) and their standard deviation (ϕ_{S2S}). $\delta S2S_s$ in the upper panel is computed with respect to Abrahamson et al. (2014), while in the lower panel it is computed with respect to Arteta et al. (2023).

For Fourier IMs, we follow the same procedure with the EAS (5 Hz), comparing it with the GMPMs of Bayless and Abrahamson (2018). Results are shown in Figure 9. Statistical values computed are shown in Figure 9 and Table 2.

We check the mean, standard deviation, and Gaussian-like shape of ε, and the Shapiro-Wilk test for normality. Residuals are Gaussian-like distributed for this dataset with respect to both GMPMs, the global and the regional developed one (Table 2 and Figures A2 and A3). The same result is determined for the Fourier IMs EAS (Table 2 and Figure A4).

https://doi.org/10.5194/essd-2026-202
Preprint. Discussion started: 15 April 2026

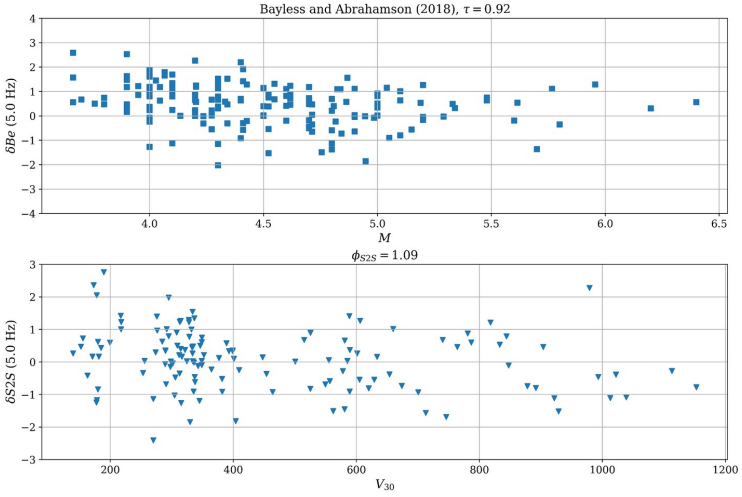

Figure 9. δB_e and $\delta S2S_s$ from the EAS (5 Hz) presented in the flatfile and the Bayless and Abrahamson (2018) GMPM. Upper panel: Between event variability (δBe) of the continental earthquakes and its standard deviation (τ). Lower panel: Site-to-site residuals (δS2S) and its standard deviation (ϕ_{S2S}).

4 Conclusions

A ground motion flatfile is presented after homogeneous preprocessing of the acceleration records following Pacor et al. (2010) and Lanzano et al. (2019) of the 8086 three-components records of 694 shallow earthquakes in Colombia, a region with several devastating earthquakes recorded in pre-instrumental and instrumental times. This flatfile is highly useful for characterizing and modeling the ground motion associated with shallow tectonic structures in the northwestern Andes, as well as to be used in any seismic hazards assessment in Northern South America or in any comparable tectonic region around the world.

A compilation of the site parameters, such as V_{S30}, H/V, and T, was carried out to constrain the characterization of the sites and their seismic response.

The dataset was validated through residual analysis with a modern and widely used GMPM of Abrahamson et al. (2014), furthermore, with a region adaptation for Northern South America of Arteta et al. (2023). For FAS data, we used the Bayless and Abrahamson (2018) GMPM for validation. We showed the Gaussian-like distribution of the dataset with the aforementioned GMPM.

The Fourier Amplitude Spectrum presented here is a powerful tool that can be used to study source parameters, such as corner frequency, seismic moment, and stress drop. In that way, moment magnitude could be computed for the whole dataset instead of the empirical relationship.

Appendix

https://doi.org/10.5194/essd-2026-202
Preprint. Discussion started: 15 April 2026

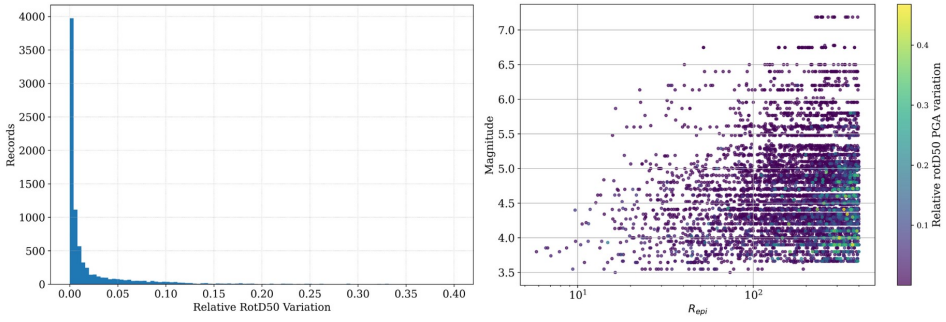

Figure A1. Sensitivity test of the low pass frequency for the bandpass filter used in the preprocessing. Lp was tested in the range 27 to 37 Hz.

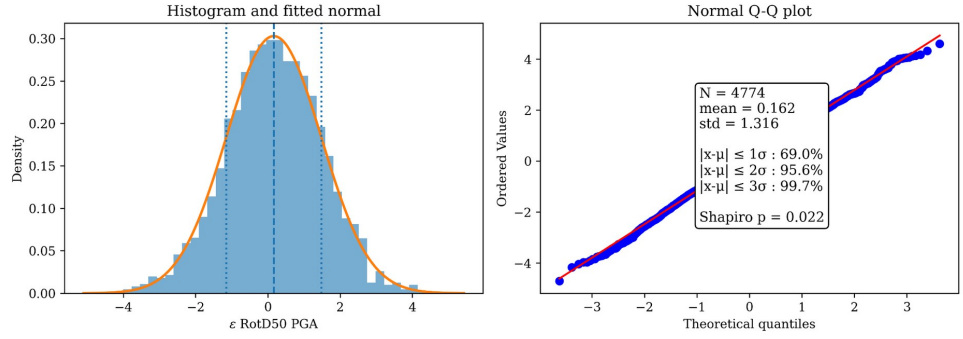

Figure A2. Basic normal analysis of the total residuals of RotD50 PGA of the dataset from the GMPM of Abrahamson et al (2014).

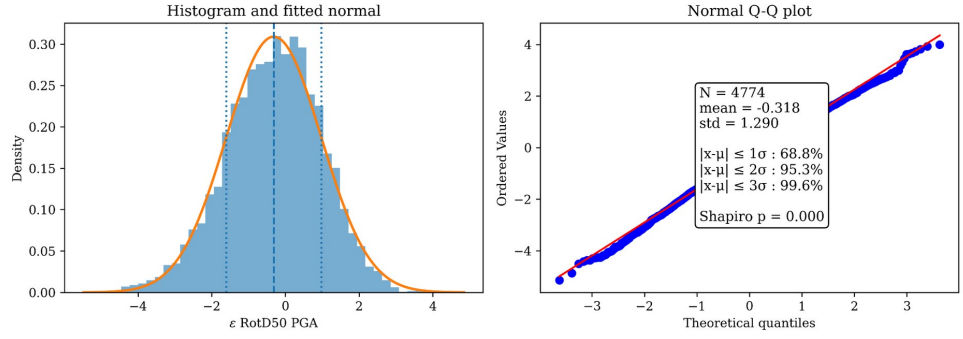

Figure A3. Basic normal analysis of the total residuals of RotD50 PGA of the dataset from the GMPM of Areta et al (2023).

https://doi.org/10.5194/essd-2026-202
Preprint. Discussion started: 15 April 2026

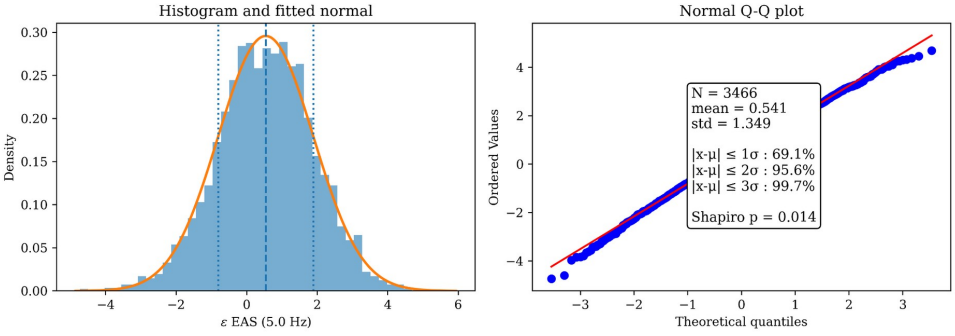

Figure A4. Basic normal analysis of the total residuals of EAS (5 Hz) of the dataset from the GMPM of Bayless and Abrahamson et al (2018).

Data availability

Data described in this manuscript can be accessed at the repository under data DOI (10.5281/zenodo.19056074, Martinez et al 2026).

Acceleration records are available on the SGC website https://catalogo-aceleraciones.sgc.gov.co/, or via FDSN: https://www.fdsn.org/networks/detail/CM/.

Author contribution

D Martinez-Jaramillo: Conceptualization, formal analysis, software, validation, writing original draft.
S.R Kotha: Conceptualization, formal analysis, software, validation, writing original draft.
F.R. Zúñiga: Validation, funding acquisition, writing review and editing.
P. Lacan: Validation, funding acquisition, writing review and editing.

Competing interest

The authors declare that they have no known competing financial interests or personal relationships that could have appeared to influence the work reported in this paper.

Acknowledgments: The acceleration time series were given by SGC under request, but also available at: https://catalogo-aceleraciones.sgc.gov.co.

Financial support: Daniel Martinez-Jaramillo is doctoral student of the Earth Sciences Graduate School, Universidad Nacional Autónoma de México and has received a SECIHTI scholarship. Partial support was received from the France-Mexico collaborative project SEP-CONACYT-ANUIES-ECOS Nº321193.

References:

Abrahamson, N. A. and Silva, W. J.: Empirical response spectral attenuation relations for shallow crustal earthquakes, Seismol. Res. Lett., 68, 94–127, 1997.

Abrahamson, N. A., Silva, W. J., and Kamai, R.: Summary of the ASK14 ground motion relation for active crustal regions, Earthquake Spectra, 30, 1025–1055, 2014.

Akkar, S., Sandıkkaya, M. A., Şenyurt, M., Azari Sisi, A., Ay, B. Ö., Traversa, P., and Godey, S.: Reference database for seismic ground-motion in Europe (RESORCE), Bull. Earthquake Eng., 12, 311–339, 2014.

https://doi.org/10.5194/essd-2026-202
Preprint. Discussion started: 15 April 2026

Ancheta, T., Bozorgnia, Y., Darragh, R., Silva, W. J., Chiou, B., Stewart, J. P., and Atkinson, G. M.: PEER NGA-West2 database: A database of ground motions recorded in shallow crustal earthquakes in active tectonic regions, Proceedings, 15th world conference on earthquake engineering, 24–28, 2012.

Arteta, C. A., Pajaro, C. A., Mercado, V., Montejo, J., Arcila, M., and Abrahamson, N. A.: Ground-motion model (GMM) for crustal earthquakes in Northern South America (NoSAm crustal GMM), Bull. Seismol. Soc. Am., 113, 186–203, 2023.

Arteta, C. A., Pajaro, C. A., Mercado, V., Montejo, J., Arcila, M., and Abrahamson, N. A.: Ground-motion model for subduction earthquakes in northern South America, Earthquake Spectra, 37, 2419–2452, 2021.

Bindi, D., Kotha, S. R., Weatherill, G., Lanzano, G., Luzi, L., and Cotton, F.: The pan-European engineering strong motion (ESM) flatfile: consistency check via residual analysis, Bull. Earthquake Eng., 17, 583–602, 2019.

Boore, D. M.: Orientation-independent, nongeometric-mean measures of seismic intensity from two horizontal components of motion, Bull. Seismol. Soc. Am., 100, 1830–1835, 2010.

Buscetti, M., Traversa, P., Perron, V., Rischette, P., Hollender, F., and Shible, H.: Epos-France Database of Earthquake Ground Motion for Mainland France: 1996–2021 Updated Version, Seismol. Res. Lett., 96, 1214–1226, https://doi.org/10.1785/0220240053, 2024.

Dawood, H. M., Rodriguez-Marek, A., Bayless, J., Goulet, C., and Thompson, E.: A flatfile for the KiK-net database processed using an automated protocol, Earthquake Spectra, 32, 1281–1302, 2016.

Ekström, G., Nettles, M., and Dziewonski, A. M.: The global CMT project 2004-2010: Centroid-moment tensors for 13,017 earthquakes, Phys. Earth Planet. Inter., 200–201, 1–9, https://doi.org/10.1016/j.pepi.2012.04.002, 2012.

Eraso, J. and Montejo, J.: Mapa de Vs30 Integrado para Colombia, Servicio Geológico Colombiano, Bogotá, 2019.

Goulet, C. A., Kishida, T., Ancheta, T. D., Cramer, C. H., Darragh, R. B., Silva, W. J., and Youngs, R. R.: PEER NGA-east database, Earthquake Spectra, 37, 1331–1353, 2021.

International Seismological Centre: ISC-EHB dataset [data set], https://doi.org/10.31905/PY08W6S3, 2025.

Kottke, A., Abrahamson, N. A., Boore, D. M., Bozorgnia, Y., Goulet, C. A., Holleback, J., Kishida, T., Der Kiureghian, A., Ktenidou, O.-J., Kuehn, N., Rathje, E. M., Silva, W. J., Thompson, E., and Wang, X.: Selection of random vibration procedures for the NGA East Project, PEER Report No. 2018/05, Pacific Earthquake Engineering Research Center, University of California, Berkeley, CA, 2018.

Lanzano, G., Sgobba, S., Luzi, L., Pacor, F., Puglia, R., Felicetta, C., and D'amico, M.: The pan-European Engineering Strong Motion (ESM) flatfile: comparison with NGA-West2 database, Boll. Geofis. Teor. Appl., 61, 2020.

Marín-Arias, J. P., Valencia Munoz, L. Y., and Rendon Cardona, L. M.: Macroseismic analysis of Murindo earthquake, Antioquia (Colombia) October 1992, Boletin de Geologia, 31, 2009.

Marín-Arias, J. M., González, H. C., and Hurtado, E. D. J. S.: Modelo geométrico del foco del terremoto de Popayán (Colombia) a partir de datos macrosísmicos, Boletín de Geología, 28, 93–109, 2006.

Martinez-Jaramillo, D., Kotha, S. R., Zúñiga, F. R., and Lacan, P.: Colombian Ground Motion: SA and FAS [data set], Zenodo, https://doi.org/10.5281/zenodo.19056074, 2026.

https://doi.org/10.5194/essd-2026-202
Preprint. Discussion started: 15 April 2026

Minson, S. E. and Dreger, D. S.: Stable inversions for complete moment tensors, Geophys. J. Int., 2, 585–592, https://doi.org/10.1111/j.1365-246X.2008.03797.x, 2008.

Montejo, J., Arcila Rivera, M. M. M., and Zornosa, D. G.: Integrated Seismic Catalog for Colombia, Boletín Geológico, 50, https://doi.org/10.32685/0120-1425/bol.geol.50.1.2023.665, 2023.

Mosquera-Machado, S., Lalinde-Pulido, C., Salcedo-Hurtado, E., and Michetti, A. M.: Ground effects of the 18 October 1992, Murindo earthquake (NW Colombia), using the Environmental Seismic Intensity Scale (ESI 2007) for the assessment of intensity, Geol. Soc. Spec. Publ., 316, 2009.

Oliveti, I., Faenza, L., and Michelini, A.: Intensity-ground motion dataset for Italy (INGe), version 2.0 [data set], Zenodo, https://doi.org/10.13127/inge.2, 2021.

Pacor, F., Felicetta, C., Lanzano, G., Sgobba, S., Puglia, R., D'Amico, M., Russo, E., Baltzopoulos, G., and Iervolino, I.: NESS v1.0: A worldwide collection of ground-motion data to investigate near source effects, Seismol. Res. Lett., https://doi.org/10.1785/0220180149, 2018.

Pájaro, C. A., Arteta, C. A., Mercado, V., Montejo, J., Arcila, M., and Abrahamson, N. A.: Partially non-ergodic ground motion model for the Bucaramanga seismic nest in Northern South America (NoSAm Nest GMM), Bull. Earthquake Eng., 22, 3677–3702, 2024.

Paris, G. and United States Geological Survey: Map and database of Quaternary faults and folds in Colombia and its offshore regions, US Geological Survey, No. 00-0284, 2000.

Rodríguez, L., Diederix, H., Torres, E., Audemard, F., Hernández, C., Singer, A., and Yepez, S.: Identification of the seismogenic source of the 1875 Cucuta earthquake on the basis of a combination of neotectonic, paleoseismologic and historic seismicity studies, J. S. Am. Earth Sci., 82, 274–291, 2018.

SGC & GEM: Modelo Nacional de Amenaza sísmica de Colombia, Servicio Geológico Colombiano (SGC) – Grupo de Amenaza Sísmica, Fundación Global Earthquake Model (GEM), 196 pp., 2018.

Sgobba, S., Felicetta, C., Lanzano, G., Ramadan, F., D'Amico, M., and Pacor, F.: NESS2.0: An Updated Version of the Worldwide Dataset for Calibrating and Adjusting Ground-Motion Models in Near Source, Bull. Seismol. Soc. Am., https://doi.org/10.1785/0120210080, 2021.

Strasser, F. O., Arango, M. C., and Bommer, J. J.: Scaling of the source dimensions of interface and intraslab subduction-zone earthquakes with moment magnitude, Seismol. Res. Lett., 81, 941–950, 2010.

Vanneste, K., Onvani, M., Rapagnani, G., and Van Noten, K.: The BELSHAKE Database of Earthquake Ground Motion in Belgium, Seismol. Res. Lett., 97, 918–933, https://doi.org/10.1785/0220250321, 2026.

Vargas-Jiménez, C. A. and Monsalve-Jaramillo, H.: 3D velocity structure around the source area of the Armenia earthquake: 25 January 1999, Mw= 6.2 (Colombia), Bol. Soc. Geol. Mex., 61, 339–351, 2009.

Wells, D. L. and Coppersmith, K. J.: New empirical relationships among magnitude, rupture length, rupture width, rupture area, and surface displacement, Bull. Seismol. Soc. Am., 84, 974–1002, 1994.

Weston, J., Engdahl, E. R., Harris, J., Di Giacomo, D., and Storchak, D. A.: ISC-EHB: Reconstruction of a robust earthquake dataset, Geophys. J. Int., 214, 474–484, https://doi.org/10.1093/gji/ggy155, 2018.